5-1-1986

Experimental study of configuration mixing in intermediate excited levels of barium.

John Hunter
University of Chicago

James Keller
University of Chicago

R. Berry
University of Chicago

Experimental study of configuration mixing in intermediate excited levels of barium

John E. Hunter III, James S. Keller, and R. Stephen Berry
Department of Chemistry and The James Franck Institute, The University of Chicago, Chicago, Illinois 60637
(Received 16 October 1985)

Resonant three-photon ionization of barium, via five closely spaced excited bound states—labeled $6s\,8s\ ^1S_0$, $6p^2\ ^3P_0$, $6p^2\ ^3P_1$, $6s\,7d\ ^1D_2$, and $6p^2\ ^3P_2$—has yielded both angular distributions of energy-resolved photoelectrons and branching ratios to the $6s$, $5d$, and $6p$ configurations of Ba^+. In contrast to earlier *ab initio* and semiempirical theoretical analyses which attributed nearly pure configurations to these five bound states, our experimental findings are consistent with a significant degree of $6p^2$ character in the $6s\,8s\ ^1S_0$ and $6s\,7d\ ^1D_2$ levels, more in accord with their original configuration labels in the tables of Moore. Branching to the $6p$ states of the ion predominates in each case, and the angular distributions of the corresponding photoelectrons from the $6p^2\ ^3P_2$ and $6s\,7d\ ^1D_2$ levels are described well by a parametric theoretical model approximating these states as pure $6p^2$ configurations. For the $6s\,8s\ ^1S_0$ level, inferences based on these observations must be made cautiously because of the possibility of an "anomalously" low photoionization amplitude for the $6s\,8s$ component of the state. Available oscillator strengths suggest the possibility of configuration interaction via spin-orbit coupling. Overall, strong configuration mixing and/or mislabeling of the configurations is implied; we suggest that the choice of configurational labels for these states be reexamined.

I. INTRODUCTION

There has been great interest in recent years in the dynamics of two-electron systems. Electron correlations in autoionizing states of helium have received the most attention, though more recently the focus has shifted toward study of both bound and autoionizing states of the alkaline-earth atoms—because they represent less "exotic" systems (having much lower excitation energies) and because of their experimental tractability. Theoretical advances have been reviewed recently by Fano[1] and experimental advances by Aymar.[2] The multichannel quantum defect theory (MQDT) has enjoyed remarkable success in describing channel interactions in the high-lying bound energy range and in the autoionization region, though it encounters difficulties when extended to the low and intermediate range of the spectrum, where many of the states consist of two electrons at roughly equivalent distances from the core (i.e., with nearly equivalent effective principle quantum numbers). Some of these low- to intermediate-lying states have recently[3–5] been incorporated into the molecular picture of electron correlation, in which the approximate constants of motion are those of the vibration and rotation of the "linear triatomic molecule" formed by the two electrons and the core.[6] The configurational assignments may be important in making this correspondence[5] as well as in addressing the broader question of what model is best for describing the correlations involved—that is, whether the independent-particle model assignments are useful even as a zeroth-order approximation, or whether correlations prevent the assignment of levels to a single main configuration.

The multiphoton ionization—photoelectron spectroscopy (MPI-PES) experiments presented in this paper probe configuration interaction and the assignment of levels in the intermediate energy range of the barium spectrum. In particular, we produced (via stepwise excitation) and photoionized five states—$6s\,8s\ ^1S_0$, $6p^2\ ^3P_{0,1,2}$, and $6s\,7d\ ^1D_2$—and measured branching ratios to excited states of the remaining ion and angular distributions of the corresponding photoelectrons as a function of the alignment of the state photoionized. Similar measurements have been made previously in order to interpret channel interactions for a series of high Rydberg states all photoionized to roughly the same final-state energy.[7,8] Previously in our laboratory similar MPI-PES studies of single states have yielded information on correlation;[9,10] in particular, the $5d7s\ ^1D_2$ level was found to have significant contributions from the $6s\,nd$ and $5d\,nd$ channels.[9]

The $6s\,8s\ ^1S_0$, $6p^2\ ^3P_{0,1,2}$, and $6s\,7d\ ^1D_2$ levels under consideration here were all originally given the configuration label $6p^2$ in the tables of Moore.[11,12] The $^1D_2$ level at 35 344 cm^{-1} was subsequently reassigned as $6s7d$ based on the MQDT analysis of the bound even-parity $J=2$ spectrum of barium,[13] which interpreted this level as having 87% contribution from the $6s\,nd\ ^1D_2$ channel but only 6% from the $6p\,np\ ^1D_2$ channel; the $6p^2$ label was assigned[13] to a higher $^1D_2$ level at 38 556 cm^{-1}. The analysis was particularly complicated in this intermediate region of the spectrum where there are more perturbers than there are members of the relevant Rydberg series; the new assignments have already been questioned by Wynne and Armstrong,[14] and, more recently, by van Leeuwen and Hogervorst.[15] Rubbmark *et al.*[16] assigned to the $^1S_0$ level its currently accepted label $6s8s$, and this assignment was supported by the MQDT analysis of Aymar *et al.*[17] which interpreted the $6s\,8s\ ^1S_0$ level as having 97.5% contribution from the $6s\,ns$ channel. Considerable controversy then arose over where the $6p^2\ ^1S_0$ level lies. The $6p^2\ ^1S_0$ label was given to states of higher and higher ener-

gy[14,16,17] until its latest assignment[18] was made to a broad autoionizing resonance at 44 800 cm^{-1}. The findings of the MQDT analyses are consistent with two earlier *ab initio* calculations: a configuration-interaction calculation by Friedrich and Trefftz[19] which indicated the predominance of the channels $6s\,ns$ and $6s\,nd$ in the $6s8s\ ^1S_0$ and $6s7d\ ^1D_2$ states respectively, and a multiconfiguration Dirac-Fock (relativistic) calculation by Rose *et al.*[20] which predicted the $6p^2\ ^1S_0$ and $^1D_2$ to lie at higher energies. The MQDT analyses indicated no perturbing effect of the nearby $6p^2\ ^3P_0$ and $6p^2\ ^3P_2$ levels, and in fact the $^3P_0$ level was interpreted to be a nearly pure (99.9%) single configuration state.[17] Because of the lack of apparent energy perturbations, certain simplifying assumptions were made which greatly reduced the number of free parameters in these analyses and thus made it possible to extract considerable information about higher-lying levels. It must be emphasized, however, as has been pointed out by Aymar,[2] that a good fit of energy levels alone is necessary but not sufficient to demonstrate that a proper description of the channel interactions has been achieved. Thus experiments such as ours are needed to provide more stringent tests of phenomenological MQDT fits.

II. EXPERIMENTAL

Details of our experimental procedure for determining angular distributions of photoelectrons from MPI-PES have been given previously,[10,21–23] so only those particular to the present experiments will be given here. A twin NRG nitrogen laser (337.1 nm) producing 5-ns pulses was used to pump two homemade dye lasers and to photoionize excited atomic states. In all these experiments a two-step excitation was performed (see Fig. 1), beginning with excitation of the $6s6p\ ^3P_1^o$ state (791.1 nm) with the dyes Oxazine 750 and 1,3,3,1′,3′,3′-hexamethyl indotricarbocyanine perchlorate (HITC) in dimethylformamide (6:1 molar ratio). Subsequent excitations to the $6p^2\ ^3P_{0,1,2}$ (457.4, 450.6, and 435.0 nm), the $6s8s\ ^1S_0$ (460.0 nm), and the $6s7d\ ^1D_2$ (440.3 nm) states were achieved using Coumarin 450 in ethanol. Coumarin 460 was not used because its superradiance led to excitation of the Sr resonance line at 460.7 nm. (Strontium impurities in our barium samples were on the order of 1%.)

All three laser beams were plane polarized and their polarization vectors were rotated synchronously to obtain angular distributions of photoelectrons. The detector was fixed on an axis perpendicular to both the laser beams and the effusive barium beam. The nitrogen-laser beam was passed through a Glan-Thompson polarizer and a rotating 337.1-nm half-wave plate. The two dye-laser beams were passed through a beam splitter and a Glan-Thompson polarizer to achieve collinearity and parallel polarizations for the experiments involving the $J=0$ and $J=2$ states. For the $6p^2\ ^3P_1$ experiment, crossed polarization of the excitation beams was necessary in order to reach this $J=1$ state. In this case, the dye beams were sent through a quartz Wollaston prism, which split each beam into horizontally and vertically polarized components; adjustment of incident beam angles made the appropriately polarized component beams collinear. In all cases a rotating double

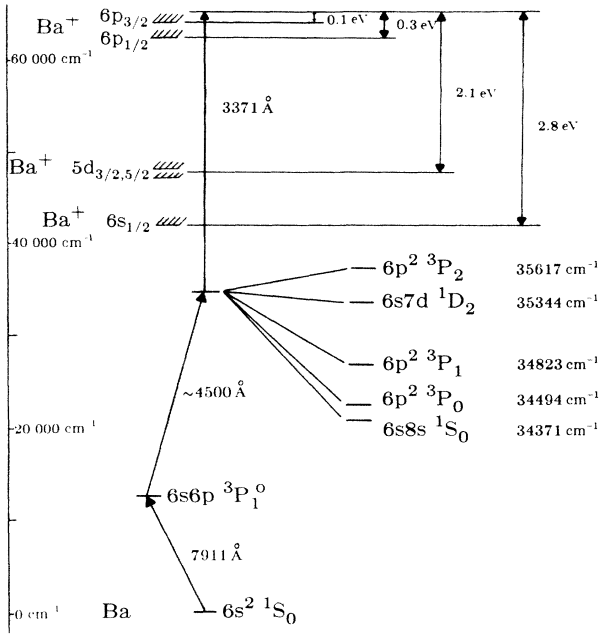

FIG. 1. Simplified energy-level diagram of barium showing those levels which are relevant to our experiments.

Fresnel rhomb was used to rotate the polarization vectors of the dye-laser beams. The angular distributions were characterized by an adjustable angle η between the polarization directions of the uv beam (ν_3) and the second dye-laser beam (ν_2) (see Fig. 2).

A delay between the excitation pulses (ν_1 and ν_2) of 4–9 ns eliminated photoionization of the excited state by the first dye-laser beam ($\nu_1+\nu_2+\nu_1$). The second dye-laser beam was attenuated to eliminate ionization by a

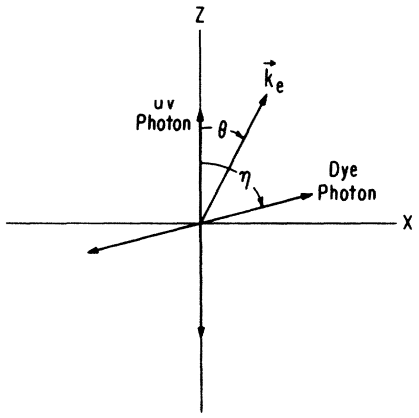

FIG. 2. Schematic of the system geometry. The three collinear plane-polarized laser pulses, which propagate out of the page, intersect the barium atomic beam at the origin. The polarization direction of the nitrogen-laser (photoionizing) photon defines the z axis; the plane of polarization of the second dye laser is rotated clockwise from the z axis by the angle η. The momentum vector $\mathbf{k}_e$ of the photoelectron is in the plane of the page at the angle θ measured clockwise from the z axis.

$\nu_1+\nu_2+\nu_2$ process. Direct ionization of the $6s6p\,^3P_1^o$ state ($\nu_1+\nu_3$) could not be eliminated because of the long lifetime (~ 1 μs) of this first excited state; a delay (2–4 ns) between the second dye pulse and the uv ionization pulse enhanced the desired $\nu_1+\nu_2+\nu_3$ process with respect to the $\nu_1+\nu_3$ process. The delay between ν_2 and ν_3 was restricted by the possibility of decay of the excited states and subsequent ionization by the uv laser pulse. Most of the desired electrons arrived at the detector before the $\nu_1+\nu_3$ interfering peak, but some very-low-energy electron peaks that arrived afterwards were overwhelmed by the large $\nu_1+\nu_3$ signal. The reliability of branching ratios and angular distributions of such low-energy electrons is doubtful anyway because of the presence of stray fields. The resonance transition in barium, $6s^2\,^1S_0\rightarrow 6s6p\,^1P_1^o$, was not utilized in these experiments because of weak transition strengths from the $^1P_1^o$ state to the desired higher excited states and because direct ionization of the $^1P_1^o$ state leads to severe resolution problems.

The excitation energy of the $\nu_1+\nu_2+\nu_3$ photoionization process described here was always high enough so that five states of the ion core were energetically accessible—the $6s\,^2S_{1/2}$, the $5d\,^2D_{3/2,5/2}$, and the $6p\,^2P_{1/2,3/2}$ states of Ba^+. Energy resolution was accomplished by time-of-flight analysis over a 3.8-cm field-free path on the way to the channeltron detector. Selective observation of electron groups was achieved by applying a stopping potential to a screen placed in front of the channeltron to prevent any electron transmission except during the application of a positive pulse from a pulse generator. We were able to resolve the peaks corresponding to production of the fine-structure levels of the $6p\,^2P$ term of the ion. The photoelectrons corresponding to production of the $6s\,^2S_{1/2}$ and the $5d\,^2D_{3/2,5/2}$ levels of the ion were all greater than 2 eV in energy and were spread by less than 10 ns in time at the detector position; thus these peaks were not resolved.

III. THEORY AND DATA ANALYSIS

In order to assess the degree of $6p^2$ character of the states in question, we developed a parametric theoretical expression for the angular distribution of photoelectrons, assuming a *direct* photoionization process of a $6p^2$ configuration having the given term symbol

$$6s^2\,^1S_0\rightarrow 6s6p\,^3P_1^o\rightarrow 6p^{2\,(2S+1)}L_J\rightarrow 6p\,^2P_j+\epsilon s,d\ , \tag{1}$$

where S, L, and J are respectively the total spin, total orbital, and total electronic angular momenta, and j is the total electronic angular momentum of the remaining state of the ion. This is based entirely on an independent-particle model in which the individual electron orbital angular momenta are good quantum numbers and the ionizing photon acts on only one of these, so the only allowed process leaves the ion in one of the fine-structure levels of the $6p\,^2P$ state. A similar model could have been developed for photoionization of the $6s8s$ and $6s7d$ to the $6s\,\epsilon l$ continuum. However, as we have pointed out previously,[10,23] the fit of data to such a model would give no information on the goodness of the configurational label but rather would just test the validity of the term symbol. Further, we could not resolve the $5d\,\epsilon l$ and $6s\,\epsilon l$ photoelectrons in the present experiments.

The methods for deriving such an expression using irreducible-density-matrix methods in the Liouville representation[22,24,25] have been given previously for the case of two-photon ionization.[22] The extension to the three-photon case is straightforward. The resulting expression is

$$\frac{d\sigma}{d\Omega}=\sum_{\substack{l_f,l_f',K,Q\\P_1,P_2,P_{12},P_3}}\langle\epsilon(\Omega)\,|\,(l_fl_f')K,(ss)0,(j_cj_c)0,(ii)0;KQ\rangle_L$$

$$\times\langle(l_fl_f')K,(ss)0,(j_cj_c)0,(ii)0;K||S||(ii)0,(j_aj_a)0,((11)P_1,(11)P_2)P_{12},(11)P_3;K\rangle_L$$

$$\times\langle(ii)0,(j_aj_a)0,((11)P_1,(11)P_2)P_{12},(11)P_3;KQ\,|\,\rho\rangle_L\ , \tag{2}$$

where the subscript L indicates the Liouville representation; l_f (l_f') and s are the orbital and spin angular momenta of the continuum electron; j_c and j_a are the ionic core and initial atomic electronic angular momenta; and i is the nuclear angular momentum. $|\rho\rangle$ is the initial density state and $\langle\epsilon(\Omega)|$ is the detector (efficiency) operator. P_1, P_2, and P_3 give the multipole orders (0 or 2) of the three linearly polarized photons, while K gives the multipole order of the entire system of atom and photons (i.e., the system possesses 2^K polarization). P_{12} gives the multipole order of the first two photons coupled together (which is equal to that of the state to be photoionized). By placing all nonisotropic multipole moments in the initial density state, the interactions can be represented by the composite *scalar* scattering operator S. The Liouville amplitudes in Eq. (2), corresponding to probabilities or intensities in Hilbert space, are

$$\langle\epsilon(\Omega)\,|\,(l_fl_f')K,(ss)0,(j_cj_c)0,(ii)0;KQ\rangle_L=\frac{1}{\sqrt{4\pi}}[s,j_c,i]^{1/2}(-1)^{l_f}[l_f,l_f']^{1/2}Y_{KQ}\begin{bmatrix}l_f & l_f' & K\\ 0 & 0 & 0\end{bmatrix}, \tag{3}$$

$$\langle((ii)0,(j_aj_a)0,((11)P_1,(11)P_2)P_{12},(11)P_3;KQ\,|\,\rho\rangle_L$$
$$=\sum_{M_1,M_2}[i,j_a]^{-1/2}\langle(11)P_1M_1\,|\,\rho_1\rangle\langle(11)P_2M_2\,|\,\rho_2\rangle\langle P_1M_1P_2M_2\,|\,P_{12}Q\rangle\langle(11)P_30\,|\,\rho_3\rangle\langle P_{12}QP_30\,|\,KQ\rangle\ , \tag{4}$$

$$\langle((l_fl_f')K,(ss)0,(j_cj_c)0,(ii)0;K||S||(ii)0,(j_aj_a)0,((11)P_1,(11)P_2)P_{12},(11)P_3;K\rangle_L$$
$$=\sum_{j_p,j_p'}W(P_1)[l_f,l_f',P_1,P_2,P_3]^{1/2}[j_c,j_p,j_p',S,L][P_{12}]^{3/2}[J]^2$$
$$\times\begin{Bmatrix}l & l & P_{12}\\ 1 & 1 & P_3\\ l_f & l_f' & K\end{Bmatrix}\begin{Bmatrix}s & l & j_p\\ s & l & j_p'\\ 0 & P_{12} & P_{12}\end{Bmatrix}\begin{Bmatrix}j_c & j_p & J\\ j_c & j_p' & J\\ 0 & P_{12} & P_{12}\end{Bmatrix}\begin{Bmatrix}s & s & S\\ l & l & L\\ j_c & j_p & J\end{Bmatrix}$$
$$\times\begin{Bmatrix}s & s & S\\ l & l & L\\ j_c & j_p' & J\end{Bmatrix}\begin{Bmatrix}1 & 1 & P_1\\ 1 & 1 & P_2\\ J & J & P_{12}\end{Bmatrix}\langle l_f||R||(l1)l_f\rangle\langle(l1)l_f'||R^\dagger||l_f'\rangle\ , \tag{5}$$

where $[j_1,j_2]=(2j_1+1)(2j_2+1)$, etc.; $\langle l_f||R||(l1)l_f\rangle$ is the reduced matrix element of Hilbert space; $l\,(=1)$ is the orbital angular momentum of the individual electrons in the $6p^2$ state formed after absorption of two photons; and j_p (j_p') is the total angular momentum of the electron to be photoionized. $W(P_1)$ accounts for the hyperfine interaction in the intermediate state. The form of the reduced matrix element is quite analogous to that used in a previous paper [Ref. 10, Eq. (6)]. Here the quantum numbers have been left as symbols to make the expression more transparent and general. The general form of the resulting angular distribution is given by

$$\frac{d\sigma}{d\Omega}=C_{00}P_{00}+C_{20}P_{20}+C_{21}P_{21}+C_{22}P_{22}$$
$$+C_{40}P_{40}+C_{41}P_{41}+C_{42}P_{42}\ , \tag{6}$$

where the P_{LM} are associated Legendre polynomials with argument $\cos\theta$; θ is the angle between the momentum vector of the photoelectron and the polarization axis of the ionizing photon. The small effect of the hyperfine structure has been included only in the $6s6p\ ^3P_1^o$ intermediate state. Since the hyperfine precession time is small compared with the laser pulse duration, the effect is characterized by a single constant parameter Z, the calculation of which has been outlined previously.[23] In short, Z (0.87 for this case) gives a measure of how much of the alignment due to the first photon is retained, when some part is lost to the (unobserved) nuclear spin space via the hyperfine interaction. The angle η determines the alignment (in the laboratory frame) of the state photoionized. The phenomenological coefficients C_{LM} determined using Eqs. (2)–(5) are functions of the angle η and of Z as well as of the fitted microscopic parameters σ_s, σ_d, and $\cos(\delta_s-\delta_d)$, where δ_l and σ_l represent, respectively, the phase shift of the l partial wave and the radial matrix element for the transition $6p\rightarrow\epsilon l$. The corresponding coefficients for photoionization of a $6p^2\ ^1D_2$ level leaving the ion in the $^2P_{3/2}$ state are

$$C_{00}=\tfrac{1}{54}\sigma_s^2[14Z+34-3(5Z+7)\sin^2\eta]$$
$$+\tfrac{1}{270}\sigma_d^2[50Z+214-3(5Z+7)\sin^2\eta]\ ,$$
$$C_{20}=-\tfrac{2}{27}\sigma_d\sigma_s\cos(\delta_s-\delta_d)[14Z+34-3(5Z+7)\sin^2\eta]$$
$$+\tfrac{1}{378}\sigma_d^2[106Z+350-15(5Z+7)\sin^2\eta]\ ,$$
$$C_{21}=-[\tfrac{1}{18}\sigma_s\sigma_d\cos(\delta_s-\delta_d)-\tfrac{1}{63}\sigma_d^2](5Z+7)\sin(2\eta)\ ,$$
$$C_{22}=\tfrac{1}{84}\sigma_d^2(5Z+7)\sin^2\eta\ , \tag{7}$$
$$C_{40}=\tfrac{2}{35}\sigma_d^2[10Z+14-3(5Z+7)\sin^2\eta]\ ,$$
$$C_{41}=\tfrac{1}{35}\sigma_d^2(5Z+7)\sin(2\eta)\ ,$$
$$C_{42}=\tfrac{1}{210}\sigma_d^2(5Z+7)\sin^2\eta\ .$$

These coefficients are exactly twice those for the process $6p^2\ ^1D_2\rightarrow 6p\ ^2P_{1/2}+\epsilon s,d$ and four times those for the process $6p^2\ ^3P_2\rightarrow 6p\ ^2P_{1/2}+\epsilon s,d$. The coefficients corresponding to $6p^2\ ^3P_2\rightarrow 6p\ ^2P_{3/2}+\epsilon s,d$ are given by

$$C_{00}=-\tfrac{1}{54}\sigma_s^2[5Z-11-3(5Z+7)\sin^2\eta]$$
$$+\tfrac{1}{270}\sigma_d^2[40Z+236+3(5Z+7)\sin^2\eta]\ ,$$
$$C_{20}=\tfrac{2}{27}\sigma_s\sigma_d\cos(\delta_s-\delta_d)[5Z-11-3(5Z+7)\sin^2\eta]$$
$$+\tfrac{5}{378}\sigma_d^2[4Z+56+3(5Z+7)\sin^2\eta]\ ,$$
$$C_{21}=[\tfrac{1}{18}\sigma_s\sigma_d\cos(\delta_s-\delta_d)-\tfrac{1}{63}\sigma_d^2](5Z+7)\sin(2\eta)\ ,$$
$$C_{22}=-\tfrac{1}{84}\sigma_d^2(5Z+7)\sin^2\eta\ , \tag{8}$$
$$C_{40}=-\tfrac{2}{35}\sigma_d^2[10Z+14-3(5Z+7)\sin^2\eta]\ ,$$
$$C_{41}=-\tfrac{1}{35}\sigma_d^2(5Z+7)\sin(2\eta)\ ,$$
$$C_{42}=-\tfrac{1}{210}\sigma_d^2(5Z+7)\sin^2\eta\ .$$

All of the coefficients in Eqs. (7) and (8) have been multi-

plied by a constant factor of 9 for simplification. We do not list the coefficients resulting from Eqs. (2)—(5) for photoionization of the $J=0$ and $J=1$ states since these were not used in our data analysis. Some aspects of these expressions are discussed in Sec. IV.

The experimentally determined angular distributions of electrons from photoionization of the two $J=2$ states (leaving the ion in one of the fine-structure levels of the ^2P state) are given in Figs. 3 and 4. The curves represent fits to the $6p^2$ single-configuration model described above.

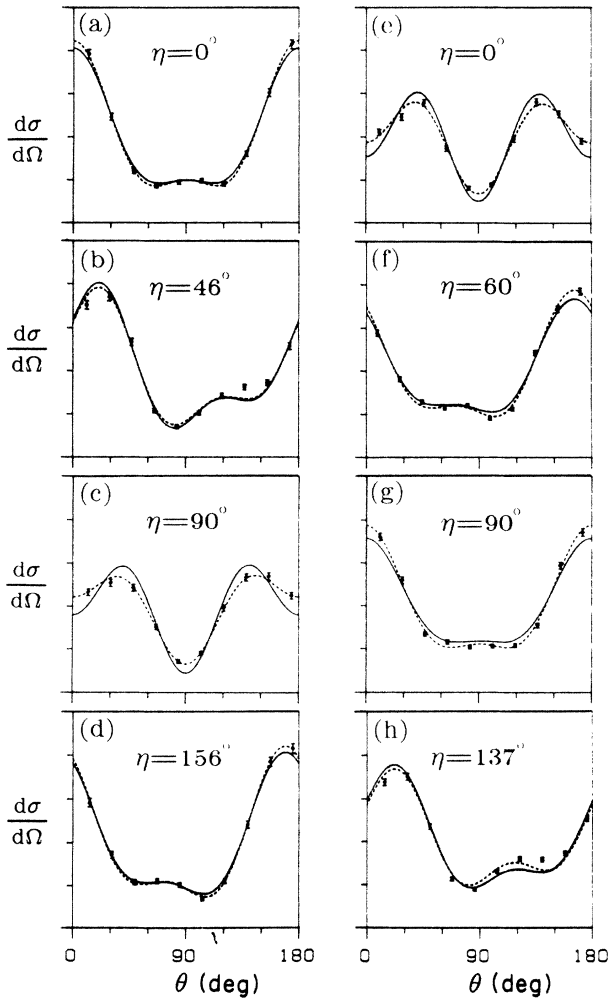

FIG. 3. Angular distributions of photoelectrons resulting from the process $6s^2\,{}^1S_0 \rightarrow 6s6p\,{}^3P_1^o \rightarrow 6p^2\,{}^3P_2 \rightarrow 6p\,{}^2P_j + \epsilon s,d$ for different values of η. The curves (a)—(d) correspond to production of the $6p\,{}^2P_{1/2}$ state of the ion and (e)—(h) to production of the $6p\,{}^2P_{3/2}$ state. Ten data points, shown with error bars, define the angular distributions. The horizontal scale is the angle θ between the z axis and the electron momentum vector $\mathbf{k}_e$ (see Fig. 2), and the vertical scale is the differential cross section in arbitrary units; all distributions are normalized to total counts, so the vertical scales are consistent with one another. The dashed curves represent the least-squares fit of each individual distribution to the $6p^2$ configurational model; the solid curves represent the expected distributions based on the average values of the microscopic parameters determined from the individual fits for each of the two families of curves shown here.

The dashed curves are determined from the least-squares fit of the data for each individual distribution to Eq. (6), with the coefficients C_{LM} given by the appropriate expressions [Eq. (7) or (8)]. The solid curves represent the expected distributions based on the average values of the microscopic parameters from the entire family of distributions (different values of η) for the particular state photoionized and remaining fine-structure level of the ion. The values of these parameters are listed in Table I.

For $\eta=0°$ or 90°, Eq. (6) can be simplified to

$$\frac{d\sigma}{d\Omega} = C_{00}P_{00} + C_{20}P_{20} + C_{40}P_{40} \,. \tag{9}$$

The angular distributions of electrons from photoionization of the $J=0$ and $J=1$ states are shown in Fig. 5. The fitted curves correspond to least-squares fits of the data to Eq. (9) with coefficients unconstrained by the $6p^2$ model: a term $C_{60}P_{60}$ was added for the fitting, as dis-

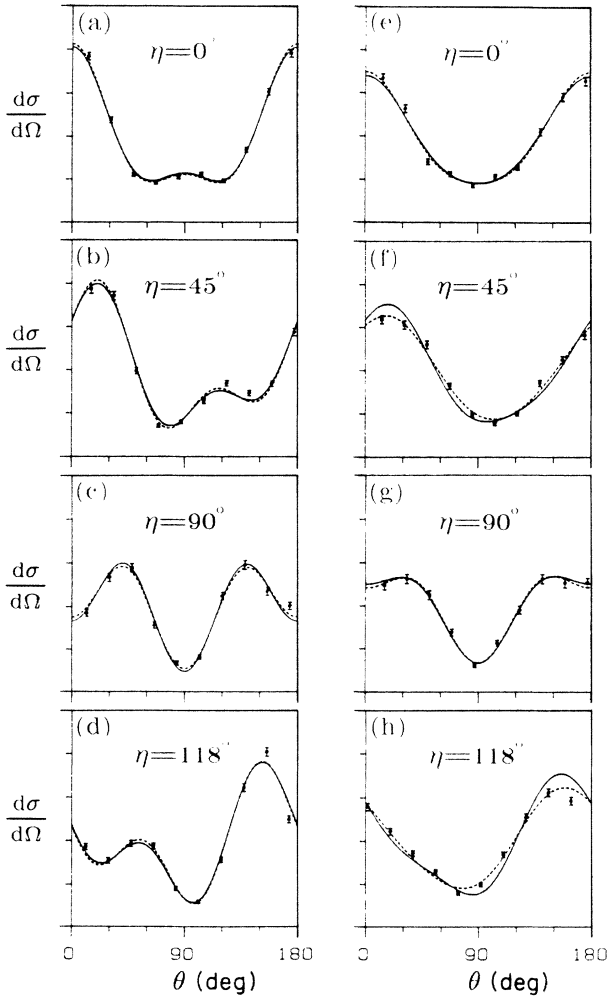

FIG. 4. Angular distributions of photoelectrons resulting from the process $6s^2\,{}^1S_0 \rightarrow 6s6p\,{}^3P_1^o \rightarrow 6s7d\,{}^1D_2 \rightarrow 6p\,{}^2P_j + \epsilon s,d$ for different values of η. The curves (a)—(d) correspond to production of the $6p\,{}^2P_{1/2}$ state of the ion and (e)—(h) to production of the $6p\,{}^2P_{3/2}$ state. As in Fig. 3, the fits are based on the $6p^2$ configurational model.

TABLE I. The microscopic parameters—the magnitudes of σ_s/σ_d and $\cos(\delta_s-\delta_d)$, and the sign of their product—as determined from the fit of the data to the $6p^2$ configurational model.

State photoionized	Ion state left	$\lvert\sigma_s/\sigma_d\rvert$	$\lvert\cos(\delta_s-\delta_d)\rvert$	$\mathrm{sgn}[(\sigma_s/\sigma_d)\cos(\delta_s-\delta_d)]$
$6p^2\,^3P_2$	$6p_{1/2}$	1.10±0.40	0.28±0.09	−1
	$6p_{3/2}$	1.74±0.47	0.30±0.09	−1
$6s7d\,^1D_2$	$6p_{1/2}$	0.96±0.17	0.17±0.04	−1
	$6p_{3/2}$	2.76±1.33	0.65±0.27	−1

cussed in Sec. IV. The resulting phenomenological parameters are listed in Table II along with those obtained in a similar fashion for the $J=2$ states.

IV. RESULTS AND DISCUSSION

Our experimentally determined branching ratios to the energetically accessible states of the remaining ion for photoionization of the $6s8s\,^1S_0$, $6p^2\,^3P_{0,1,2}$, and $6s7d\,^1D_2$ levels are presented in Table III. We observed no dependence of the branching ratios on η. That photoionization of each of the $6p^2\,^3P$ levels gives greater than 85% branching to the $6p$ states of the ion is certainly consistent with their configuration label. However, direct photoionization of a barium atom in a *pure* $6s8s$ or $6s7d$ configuration to the final-state energy we reached should yield a $6s\,\epsilon l$ final state. Thus the large branching we observed to the $6p$ configuration of the ion in these cases, comparable to that for photoionization of the $6p^2\,^3P$ levels, suggests a substantial admixture of the $6p^2$ configuration in the so-called $6s8s\,^1S_0$ and $6s7d\,^1D_2$ levels, in contrast to the findings of the semiempirical and *ab initio* theoretical studies mentioned in the Introduction. The branching to the $6p$ configuration is so dominant that it suggests that $6s8s$ and $6s7d$ *may* be improper labels for these levels.

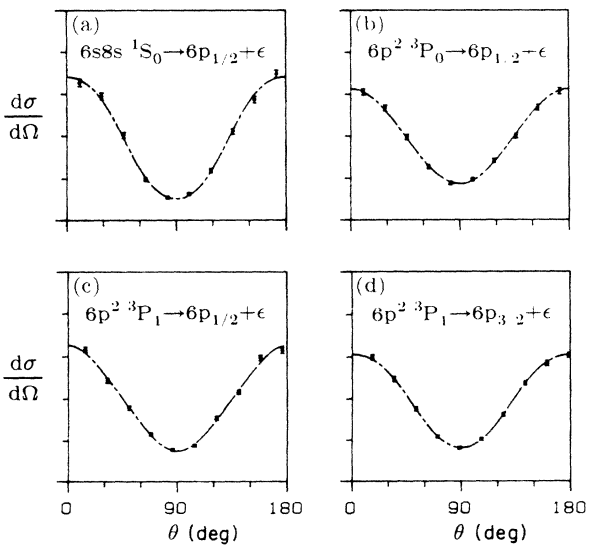

FIG. 5. Angular distributions of photoelectrons from photoionization of the (a) $6s8s\,^1S_0$; (b) $6p^2\,^3P_0$; (c), (d) $6p^2\,^3P_1$ levels of barium. The curves represent least-squares fits of the data to Eq. (9) with unconstrained coefficients. In each case $\eta=0°$.

Before drawing conclusions, however, we must note that the branching ratios do not reflect *directly* the configurational composition of the given state being photoionized since they depend on the transition amplitude for photoionization of each particular configurational component of the state to the particular final state as well as on the configurational composition itself. Calculations by Aymar[26] using a simple central-field model indicate that all of the relevant photoionization amplitudes are comparable for the $6s7d\,^1D_2$ level and thus suggest that our observed branching ratio is indeed due to a large degree of $6p^2$ mixing. For the $6s8s\,^1S_0$ level, on the other hand, the calculations indicate that the $8s\rightarrow\epsilon p$ transition is so weak at our final-state energy that even a very small admixture of $6p^2$ character could lead to significant branching to the $6p$ state of the ion.

We must also consider the possibility that interactions in the continuum influence the branching ratios. The likelihood of such interactions is small because the total energy of the final state we reached is ~ 19000 cm^{-1} below the next higher ionization limit (Ba^+ $7s\,^2S_{1/2}$). Low-resolution synchrotron scans[27,28] have shown no resonance structure in this region, though broad and weak features could have been missed and only $J=1$ resonances would be accessible to this single-photon approach. A Hartree-Fock calculation[29] has put the $7s7p\,^{1,3}P^o$ autoionizing resonances at ~ 4000 and ~ 6000 cm^{-1} above the final-state energies we reached. Finally, $J=2$ resonances could not have been excited for $\eta=0°$ in the photoionization of the two $J=2$ levels.

It clearly would be desirable to carry out an experiment similar to ours, going through the $6s7d\,^3D_2$ level, which is near in energy to the states we studied. Insofar as this term symbol is good, one would expect the predominant branching to go to the $6s$ configuration of the ion, even allowing for configuration mixing, since there is no ^3D term arising from a $6p^2$ configuration. We were unable to accomplish this experiment because the laser power necessary to pump the transition to the $6s7d\,^3D_2$ level was high enough to cause its photoionization (i.e., a $\nu_1+\nu_2+\nu_2$ process), thus competing somewhat with the nitrogen laser in the photionization step. A more powerful ionizing laser would be needed to carry out this experiment.

The angular distributions of photoelectrons corresponding to production of the $6p\,^2P_{1/2}$ and $^2P_{3/2}$ states of the ion from photoionization of the $6p^2\,^3P_2$ and $6s7d\,^1D_2$ lev-

TABLE II. Phenomenological parameters obtained from least-squares fits of the angular distributions of photoelectrons for $\eta=0°$ and 90° to Eq. (9) with normalization determined by setting $C_{00}=1$.

State photoionized	Ion state left	η	C_{20}	C_{40}	C_{60}
$6s8s\ ^1S_0$	$6p_{1/2}$	0°	1.30±0.04	0.01±0.04	−0.03±0.05
		90°	1.27±0.04	−0.02±0.05	−0.01±0.06
$6p^2\ ^3P_0$	$6p_{1/2}$	0°	0.92±0.05	−0.01±0.02	−0.01±0.05
		90°	0.89±0.05	−0.00±0.04	−0.01±0.06
$6p^2\ ^3P_1$	$6p_{1/2}$	0°	1.04±0.04	−0.03±0.04	0.02±0.04
		90°	1.07±0.04	0.03±0.04	0.03±0.04
	$6p_{3/2}$	0°	0.97±0.02	−0.05±0.03	−0.01±0.04
		90°	0.95±0.08	0.00±0.02	−0.02±0.02
$6p^2\ ^3P_2$	$6p_{1/2}$	0°	1.16±0.03	0.79±0.01	0.08±0.10
		90°	0.83±0.01	−0.54±0.08	0.01±0.06
	$6p_{3/2}$	0°	0.72±0.03	−0.69±0.02	0.05±0.03
		90°	1.01±0.03	0.56±0.02	0.03±0.04
$6s7d\ ^1D_2$	$6p_{1/2}$	0°	1.06±0.03	0.77±0.04	−0.01±0.07
		90°	0.77±0.01	−0.84±0.05	0.06±0.08
	$6p_{3/2}$	0°	0.96±0.05	0.20±0.12	−0.04±0.03
		90°	0.89±0.05	−0.36±0.09	0.01±0.05

els are both fit quite well by the simple independent-particle models based on photoionization of $6p^2\ ^3P_2$ and $^1D_2$ levels as presented in Sec. III (see Figs. 3 and 4). This is certainly consistent with a substantial amount of $6p^2$ character in the $^1D_2$ state. Independent of any fit to parameters, the $6p^2$ configurational model predicts the correct sign for the coefficient of P_{40} in each case for both $\eta=0°$ and 90°, and predicts the rough experimental observation that the C_{40} coefficients should be equal in magnitude and opposite in sign for $\eta=0°$ and 90°. The only indication of significant difficulties with the simple model we employed is the unexpectedly large difference between the fitted values of σ_s/σ_d for the processes corresponding to the production of the two fine-structure levels of the ^2P state of the ion in the photoionization of the $6s7d\ ^1D_2$ level.

We were unable to obtain a unique fit to the microscopic parameters σ_s/σ_d and $\cos(\delta_s-\delta_d)$ for the angular distributions of electrons resulting from photoionization of the $J=0$ and $J=1$ levels, and thus were unable to determine any information from them regarding the validity of the configuration labels of these states. These distributions can be described essentially with a single parameter β $(=C_{20})$. Conservation of parity and total angular momentum impose certain restrictions on the phenomenological parameters, while other restrictions follow only from application of the $6p^2$ configuration model. For photoionization of both $J=0$ states the C_{4M} and C_{6M} coefficients (nonzero in the general three-photon ionization process) are zero and the C_{20} coefficients are independent of η (both to within experimental error), as they must be, according to the general conservation laws. Another model-independent consequence is that the C_{60} coefficients should also be zero, as they are, within error bars, for photoionization of the $J=1$ and the two $J=2$ states, since a g wave $(l=4)$ would be needed to produce the sixth harmonic (f wave is forbidden by conservation of parity). While general conservation laws do not prevent the angular distributions from exhibiting η dependence or fourth harmonics for the photoionization of the $J=1$ state, these phenomena were not observed. For the ionization process leading to the $6p\ ^2P_{3/2}$ state of the ion, this result comes directly from the $6p^2$ configurational model, for which the corresponding C_{4M} coefficients are identically zero for this particular case and there is no dependence on η. This may be understood by considering the jj label for the $J=1$ state $(6p_{3/2}6p_{1/2})_{J=1}$, which has a 1:1 correspondence with the LS label. In our model, production of the $6p\ ^2P_{3/2}$ state of the ion corresponds to ionization of the $6p_{1/2}$ electron which cannot be aligned (thus explaining the η independence) and whose ionization cannot yield the $\epsilon d_{5/2}$ partial wave necessary to produce the fourth harmonic.

Several pieces of evidence from earlier work are of interest here. The transitions to the levels that have been labeled $6s8s\ ^1S_0$ and $6s7d\ ^1D_2$ are stronger from the $6s6p\ ^3P_1^o$ level than from the $6s6p\ ^1P_1^o$. As estimated from a synthesis of corrected[30] experimental[31] and calculated[19]

TABLE III. Branching ratios to the states of the barium ion observed in photoionization via five excited states of barium.

State photoionized	Branching ratios to the states of Ba^+ (%)[a] 6s and 5d	$6p_{1/2}$	$6p_{3/2}$
$6p^2\ ^3P_0$	14	86	b
$6p^2\ ^3P_1$	13	33	54
$6p^2\ ^3P_2$	14	13	73
$6s8s\ ^1S_0$	25	75	c
$6s7d\ ^1D_2$	12	32	56

[a]Typical uncertainty is ±4%.
[b]20-meV electrons (unobserved).
[c]5-meV electrons (unobserved).

values, the oscillator strengths of the spin-*forbidden* transitions are greater by a factor of about 2. This suggests mixing via spin-orbit coupling with the nearby $6p^2\,{}^3P_0$ and $6p^2\,{}^3P_2$ levels (in addition to the mixing of $6s7d\,{}^1D_2$ with $6p^2\,{}^1D_2$ suggested above on the basis of the optimum fit of our angular distribution data). For the $6s7d\,{}^1D_2$ level, this is in accord with the recent interpretation by van Leeuwen and Hogervorst[15] of their polarizability data: that the $6p^2\,{}^3P_2$ and the $6s7d\,{}^1D_2$ may be strongly mixed. They also interpreted a predominantly $6p^2$ character in the $6s7d\,{}^1D_2$ level based on isotope shift data. Their results did not show a need for revision of the $6s8s\,{}^1S_0$ label.

If the state currently labeled $6s8s\,{}^1S_0$ were reassigned as $6p^2\,{}^1S_0$, what could be said regarding the state currently called $6p^2\,{}^1S_0$? No complete answer can be given at this time. However, new data are consistent with the ${}^1S_0$ assignment. We examined the broad autoionizing state currently labeled[18] $6p^2\,{}^1S_0$ and measured the angular distributions of photoelectrons from two-photon ionization via the $6s6p\,{}^1P_1^o$ level reaching final-state energies in the range of this resonance. As the wavelength of the ionizing laser is scanned over the resonance, the distributions show increasing $|\sigma_s/\sigma_d|$ values when fit to a previously used model[23] for the process ${}^1P_1^o \rightarrow {}^2S_{1/2} + \epsilon s,d$. This is as expected for autoionization from a $L=J=0$ resonance, which can only yield s-wave electrons, and thus is indeed consistent with the assignment as ${}^1S_0$; however, we are not able to interpret anything regarding its configurational label from our angular distribution data.

V. CONCLUSION

All of the results of our MPI-PES investigation appear to be in accord with the assumption of a $6p^2$ configuration for the previously labeled $6s7d\,{}^1D_2$ and $6s8s\,{}^1S_0$ levels of barium. This suggests either the possibility of extensive admixture of $6p^2$ character into these levels or that the original assignments ($6p^2\,{}^1D_2$ and $6p^2\,{}^1S_0$) given to them by Moore may have been valid. Our conclusions concerning the $6s7d\,{}^1D_2$ level are substantiated by the interpretation of other recent experimental work and by simple calculations of photoionization amplitudes, whereas there is more question concerning the interpretation of the $6s8s\,{}^1S_0$ level. Clearly other experiments (probing other parts of the wave functions) and more elaborate calculations are needed. If further analysis indicates extensive configuration mixing, it may be desirable to search for an alternative description, e.g., a collective model, perhaps based on vibrational and rotational rather than orbital quantum numbers. Improving our understanding of these intermediate-lying states is a critical step in the quest for an adequate and unified interpretation of the dynamics of two-electron systems such as barium.

ACKNOWLEDGMENT

We would like to thank Dr. M. Aymar for helpful correspondence and comments on the manuscript.

[1]U. Fano, Rep. Prog. Phys. **46**, 97 (1983).
[2]M. Aymar, Phys. Rep. **110**, 163 (1984).
[3]J. L. Krause and R. S. Berry, Phys. Rev. A **31**, 3502 (1985).
[4]J. L. Krause and R. S. Berry, J. Chem. Phys. **83**, 5153 (1985).
[5]M. E. Kellman, Phys. Rev. Lett. **55**, 1738 (1985).
[6]M. E. Kellman and D. R. Herrick, Phys. Rev. A **22**, 1536 (1980).
[7]E. Matthias, P. Zoller, D. S. Elliot, N. D. Piltch, S. J. Smith, and G. Leuchs, Phys. Rev. Lett. **50**, 1914 (1983).
[8]G. Leuchs and S. J. Smith, Phys. Rev. A **31**, 2283 (1985).
[9]O. C. Mullins, J. E. Hunter III, J. S. Keller, and R. S. Berry, Phys. Rev. Lett. **54**, 410 (1985).
[10]O. C. Mullins, R.-l. Chien, J. E. Hunter III, D. K. Jordan, and R. S. Berry, Phys. Rev. A **31**, 3059 (1985).
[11]C. E. Moore, *Atomic Energy Levels*, U. S. Natl. Bur. Stand. Circular No. 467 (U.S. GPO, Washington, D.C., 1958), Vol. III.
[12]H. N. Russell and C. E. Moore, J. Res. Natl. Bur. Stand. **55**, 299 (1955).
[13]M. Aymar and O. Robaux, J. Phys. B **12**, 531 (1979).
[14]J. J. Wynne and J. A. Armstrong, IBM J. Res. Dev. **23**, 490 (1979).
[15]K. A. H. van Leeuwen and W. Hogervorst, Z. Phys. A **316**, 149 (1984).
[16]J. R. Rubbmark, S. A. Borgström, and K. Bockasten, J. Phys. B **10**, 421 (1977).
[17]M. Aymar, P. Camus, M. Dieulin, and C. Morillon, Phys. Rev. A **18**, 2173 (1978).
[18]M. Aymar, P. Camus, and A. El-Himdy, J. Phys. B **15**, L759 (1982).
[19]H. Friedrich and E. Trefftz, J. Quant. Spectrosc. Radiat. Transfer **9**, 333 (1969).
[20]S. J. Rose, N. C. Pyper, and I. P. Grant, J. Phys. B **11**, 755 (1978).
[21]J. C. Hansen, J. A. Duncanson, Jr., R.-l. Chien, and R. S. Berry, Phys. Rev. A **21**, 222 (1980).
[22]R.-l. Chien, O. C. Mullins, and R. S. Berry, Phys. Rev. A **28**, 2078 (1983).
[23]O. C. Mullins, R.-l. Chien, J. E. Hunter III, J. S. Keller, and R. S. Berry, Phys. Rev. A **31**, 321 (1985).
[24]U. Fano, Rev. Mod. Phys. **29**, 74 (1957).
[25]M. P. Strand and R. S. Berry, J. Math. Phys. **23**, 587 (1982).
[26]M. Aymar (private communication).
[27]C. M. Brown and M. L. Ginter, J. Opt. Soc. Am. **68**, 817 (1978).
[28]E. B. Saloman, J. W. Cooper, and G. Mehlman, Phys. Rev. A **32**, 1878 (1985).
[29]W. Sandner, U. Eichmann, V. Lange, and M. Völkel, J. Phys. B **19**, 51 (1986).
[30]L. Jahreiss and M. C. E. Huber, Phys. Rev. A **31**, 692 (1985).
[31]B. M. Miles and W. L. Wiese, At. Data **1**, 1 (1969).